

Kilo-Hertz Color Particle Shadow Velocimetry (PSV)

Larry Goss¹, Jordi Esteveordal², and Jim Crafton³
Innovative Scientific Solutions, Inc., Dayton, OH 45440

Particle Shadow Velocimetry is an inline velocimetry technique that utilizes low power LEDs as the excitation source. Because of the low power requirements to produce particle shadows as compared to particle light scattering, kilo-hertz repetition rates can be easily achieved. This paper presents high-speed velocity measurement results for a cuvette flow, a cylinder in cross flow, and a heart valve. A high speed color camera in combination with an overdriven LED are used to make measurements at 1.1 kHz. The power from a one microsecond LED pulse is sufficient in the inline arrangement to produce particle shadows that can be utilized for velocimetry. The steps necessary to employ color for this technique are also discussed.

Nomenclature

d_e	=	imaged particle diameter
d_p	=	particle diameter
e	=	spacing between camera pixels
ε	=	threshold parameter
$f^\#$	=	lens f-number
M	=	Magnification factor
λ	=	wavelength of light
Z_{corr}	=	depth of correlation

I. Introduction

Particle Shadow Velocimetry¹⁻² (PSV) is a novel technique, which shares many of the attributes of microPIV³⁻⁵ and Forward Scatter PIV⁶ (fsPIV). It utilizes low-power, pulsed light sources such as LEDs to measure the displacement of seed particles in a flowfield. While this method is most applicable to liquid flows, it is also suitable for gaseous flows. Since this is a volumetric illumination technique it relies on the receiver optics to minimize the depth of measurement. Any pulsed light system can be used as the excitation source; however, LEDs are particularly well suited since they can be overdriven in a short-pulse mode to produce intense sub-microsecond light pulses. Because the technique does not rely upon weak-particle light scattering, lasers are neither necessary nor recommended for use with this approach.

The general layout of the PSV instrument is shown in Fig. 1. Light from a pulsed LED source is directed through the measurement area onto a camera (either interline- or color-camera). This inline arrangement allows the shadows produced by the particles that are suspended in the flow to be recorded along with their forward scatter. After the particle images are recorded (at two separate times), the images are processed by cross correlation analysis to obtain velocities. In most cases some preprocessing of the image is necessary to minimize the measurement volume.

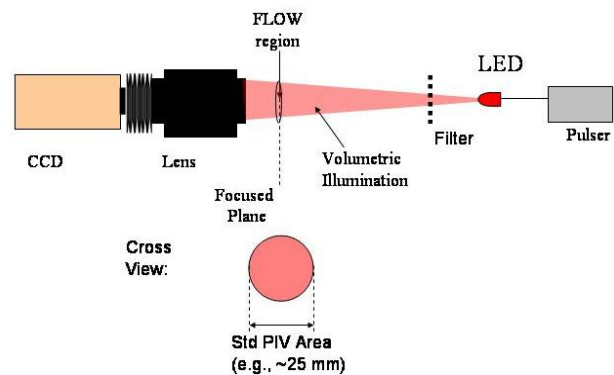


Figure 1. PSV Experimental Setup Showing Inline Excitation by LED.

¹ President, ISSI, 2766 Indian Ripple Rd., Dayton, OH 45440, Associate Fellow.

² Senior Research Engineer, ISSI, 2766 Indian Ripple Rd, Dayton OH 45440, Associate Fellow.

³ Senior Research Engineer, ISSI, 2766 Indian Ripple Rd., Dayton, OH 45440, Member

Because of the need to image individual particles, the technique is limited to small spatial-measurement regions. Since multiple pixels are required for accurate location of the particle image, it follows that

$$\frac{d_e}{e} > 1 \quad (1)$$

where d_e is the diameter of the image formed by the lens system of the particle at the camera sensor plane and e is the spacing between adjacent pixels. Adrian has shown that the diameter of the image formed by a particle located in the object plane (at focus) can be estimated by⁷

$$d_e = \left(M^2 d_p^2 + (2.44 \lambda f^\# (M + 1))^2 \right)^{1/2} \quad (2)$$

where d_p is the particle diameter, λ is the wavelength of light, M is the magnification, and $f^\#$ is the f-number of the optical system. For a typical interline-transfer camera with pixel spacing of 7 μm , f-number of 1.8, using a green LED (530 nm), accurate recording of a 1 μm size particle requires a minimum magnification of 3. Thus, the spatial area in this case is limited to approximately one-third the sensor size. For this technique cameras are required with high pixel density and small pixel size for large-area coverage.

PSV is similar to microPIV in that volumetric excitation is utilized in both techniques; however, some distinct differences should be pointed out. Epi-fluorescent microPIV techniques rely upon the laser-induced fluorescence of seed particles for the measurement of velocities. A laser is used to excite the particles and the red-shifted fluorescence is monitored through a bandpass filter to minimize interference from the laser (scattering from surfaces). The particles act as localized light sources, which--based on their location relative to the focal plane of the optics--appear as the Airy function of Fraunhofer diffraction by a circular aperture. The PSV technique relies upon particle shadows that are cast by an in-line excitation arrangement. A shift in excitation and recording wavelength is neither utilized nor desired. Also, as in the case of microPIV, surface scattering and glare present no special problems.

The particle images recorded by the PSV technique can be understood by examining the diagram in Fig. 2, which depicts the regions associated with the interaction of a plane light wave with a hard sphere. The region just downstream of the particle is called the "deep-shadow region" and is of special interest for PSV. This region is slightly smaller than the particle diameter but extends several diameters downstream. It produces an extinction cross section that is twice its geometric cross section (extinction paradox⁸). The deep shadow is surrounded by several important regions that are observed in PSV images including the Fresnel region, the diffraction rings region, and the Poisson cone. For a hard sphere, the Poisson cone has the same amplitude as the original wave, however, for a transparent sphere the amplitude can be substantially larger because of focusing of the wave by the particle. Calculations by Ovryn⁶ show that the complicated ring structure associated with the particle-wave interaction can persist for many particle diameters. This indicates that the measurement volume for the PSV technique is likely to be large compared to that of epi-fluorescence PIV.

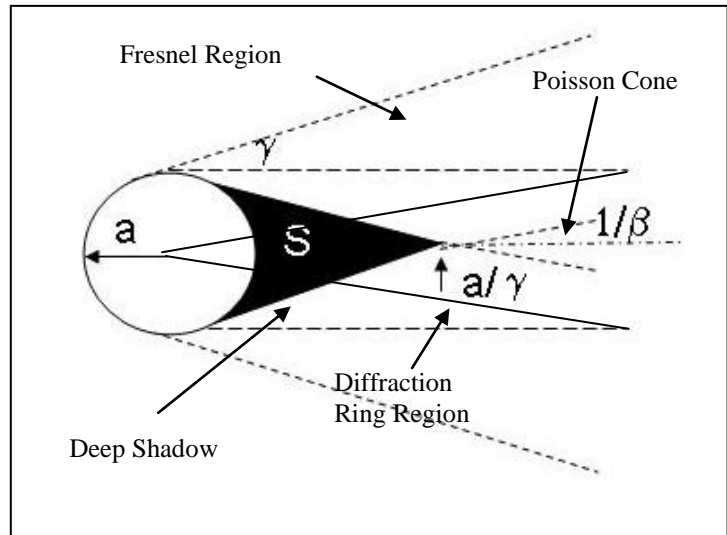


Figure 2. Depiction of Regions Associated with the Interaction of Plane Wave with Hard Sphere. S – deep shadow, a – particle radius, β – size parameter, γ – penumbra width from Nussenzweig¹⁴, 1992.

II. Measurement Depth (Depth of Correlation)

Because imaging optics are utilized for limiting the thickness of the measurement volume, it is very important to consider the effects of out-of-focus particles on the correlation results. Both Meinhart⁹ and Olsen¹⁰ have developed mathematical relationships for the depth of correlation for an epi-fluorescent PIV system. The analytical solution of

Olsen has subsequently been validated both numerically and experimentally by Bourdon¹¹. The depth of correlation is given by

$$2z_{corr} = 2 \left[\frac{(1 - \sqrt{\epsilon})}{\sqrt{\epsilon}} \left(f^{\#2} d_p^2 + \frac{5.95(M+1)^2 \lambda^2 f^{\#4}}{M^2} \right) \right]^{1/2} \quad (3)$$

where ϵ is a threshold parameter (normally set to 0.01). Note that setting the threshold parameter, ϵ , to 0.01 in the above equation is equivalent to setting the threshold parameter of Meinhart, ϕ , to 0.1. The Meinhart threshold parameter, ϕ , is the ratio of the on-axis particle intensity (at some z) to the in-focus intensity (at $z=0$). Meinhart has shown that when this ratio falls below 0.1, the particle-image intensity of the out-of-focus particle is sufficiently low that it will not influence the velocity measurement significantly.

Figure 3 depicts the PSV images of a 2.6- μm circular disk; these images are recorded at different z depths using a single LED with a 50-mm lens and standoff rings to allow a magnification of 3.5. Note that at $z = 0$ (disc located at the focal plane of the optics), the image is dominated by the deep shadow. As the focal plane is moved in front of the disc ($z = 100 \mu\text{m}$), the Poisson cone at the center of particle image becomes visible. As can be seen in both the positive and negative directions, the diffraction rings associated with the disc remain visible over a wide spatial range, indicating a large measurement depth. The line plots in Fig. 3 correspond to the normalized intensity along the image centerline. Each plot is normalized to the background light level.

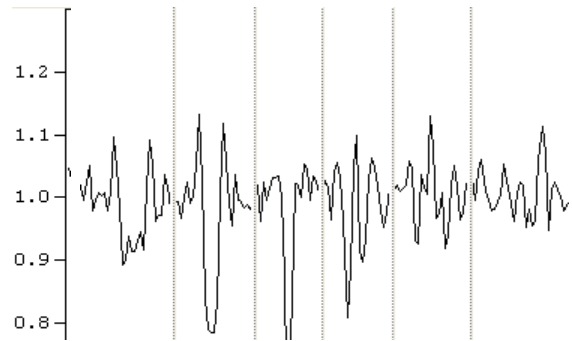
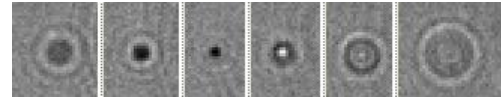


Figure 3. PSV Images of 2.6 μm Disc. Numerical units are location of focal plane from disc in μm .

The depth of correlation obtained with the PSV technique for three target discs (2.5, 5.6, and 10 μm) is shown in Fig. 4 (see upper blue line labeled no diffuser). Note that the depth of correlation in this case increases as a function of particle size and, although not shown here, is also a function of $f^{\#}$ and magnification. To compare these results with those of the epi-fluorescent case, Eq. (3) was used to calculate the depth of correlation for the same experimental parameters, i.e., $M = 3.5$ and $f^{\#} = 1.8$. The results are displayed by the lower purple line in Fig. 4 (labeled “theory”). The difference in correlation depth is large, with Eq. (3) predicting a depth of correlation that is ~ 10 times less than that observed in the PSV experiment.

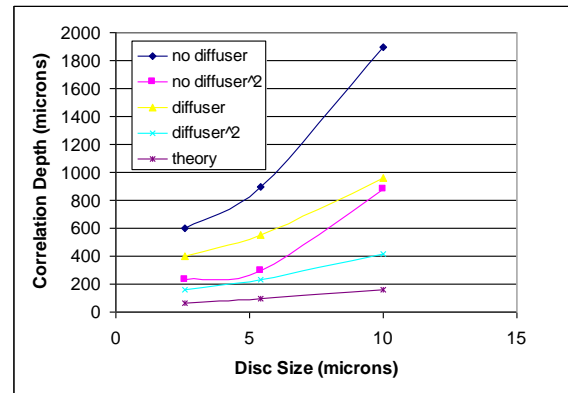


Figure 4. PSV Correlation Depth as a Function of Disc Size. $M = 3.5$ and $f^{\#} = 1.8$.

Much of the measurement depth shown in Fig. 4 is due to the partial coherence of the LED light source. Because of the relatively narrow emission lines of the LEDs, their light is partially coherent ($\Delta\lambda/\lambda = 0.025$). This increases the visibility of the diffraction rings and increases the measurement depth. One way to lower the ring visibility is to use a spatial diffuser. The spatial scrambling of the light reduces the correlation depth by nearly a factor of two (see the yellow line labeled “diffuser” in Fig. 4). An additional factor of two can be realized by squaring the PSV images as shown by Olsen¹² for the microPIV technique (see green line labeled “diffuser²” in Fig. 4). The combination of incorporating a diffuser and squaring the image reduces the correlation depth to within a factor of two of that predicted for epi-fluorescence microPIV.

To square the PSV image, it must first be inverted by subtracting it from the local average light level in the absence of a particle. The image can then be squared and processed by a standard correlation method.

III. Color PSV

Utilizing color for PSV measurements offers several advantages including: 1) the availability of low-cost, high-pixel density cameras (6-12 megapixel systems under \$2000), 2) the ability to utilize multiple colors (multiple exposures) on a single frame for velocity and acceleration measurements, and 3) the ability to utilize multiple colors in combination with multiple frames (high-speed color cameras) to increase the dynamic range for studying dynamic (transient) phenomena. However, several problems must be addressed including cross talk between color channels, color aberrations and color pixel density (most cameras have more green than red or blue pixels).

A. Color Crosstalk

To minimize color crosstalk and maximize camera sensitivity, the RGB LEDs should match the color filters of the camera. Luxeon red (650 nm), green (520 nm), and blue (470 nm) LED outputs align well with the corresponding camera filters with only a minimum amount of bleed or crosstalk with adjacent camera filters. Figure 5 shows the tri-color (RGB) LED lamp constructed for color PSV. To ensure that the output of each LED is spatially aligned, a series of dichroic filters is used to combine the LED outputs, this is important for reducing chromatic aberrations that will be discussed in the next section. Each LED has its own isolated driver electronics which allows the LEDs to be triggered independently.

B. Color Aberrations

One of the first problems encountered when working with color imaging is chromatic aberrations. Two types of aberrations are observed. Longitudinal aberrations result when the lens cannot focus the different colors in the same focal plane. In the case of LED-based PSV where volume illumination is used, the $f^\#$ cannot be increased to solve this problem. Thus, potentially three different measurement volumes are realized, i.e., the blue volume is located nearest to the lens, the red is the farthest from the lens and the green is located somewhere in between. Such an arrangement can help reduce the overall measurement volume since only the parts of the red, green, and blue volumes that are overlapped will correlate. However, this approach would lower the signal-to-noise ratio of the correlation since not all in-focus particles would correlate.



Figure 5. Tri-color RGB LED Lamp used for High Speed Color PSV Measurements.

Tangential aberrations are the sideways displacement of obliquely incident color light. This effect causes different color particle pairs to align incorrectly, resulting in a velocity bias that is a function of particle location. In fact, the magnitude of this velocity bias is a function of the wavelength difference of the two color pulses and the angular incidence of the LEDs. This fact led us to overlap the three LED outputs spatially with dichroic filters (see Fig. 5).

Methods for reducing chromatic aberrations include: 1) using color-corrected lenses, 2) using reflective optics, and 3) minimizing the spectral and spatial separation between the LEDs. The first and second methods provide workable solutions; however, they dramatically increase the cost of the system. The third method requires careful selection of the color LEDs with respect to the camera filters, overlap of the LEDs using dichroic filters, and due consideration of how to utilize the camera color-plane information. The third approach was adopted for this study.

C. Unequal Pixel Distribution

Ideally, the red, green, and blue color planes contain only information about the red, green, and blue particle images, respectively (no crosstalk between channels). This is readily achieved by matching the LED emissions to the camera color filters; however, this limits the choice of LEDs, tends to exacerbate chromatic aberrations, and does not take advantage of the camera's pixel distribution. Most color cameras utilize a Bayer¹³ color filter array in which 50% of the pixels have green filters, 25% have red, and 25% have blue.

Restricting the LEDs such that they excite only the red, green, or blue color pixels greatly reduces the number of pixels available. A four million pixel camera has only two million green pixels and one million red or blue pixels. If other than a raw image is retrieved from the camera, the camera software will produce a four million pixel RGB

image in which the missing pixel information is supplied by interpolation schemes. Unfortunately, while these schemes are very efficient, they do not accurately account for the missing data if the particle images are smaller than two-to-three pixels. In a normal color image, the human eye cannot discern the missing data. In particle imaging, however, this missing information is very important and failure to retrieve it can lead to biased and noisy velocity results.

One way to overcome this problem is to allow some crosstalk between color channels, especially with the green channel. Allowing crosstalk can increase the blue- or red-channel pixel density from 25% to 75%. The question now becomes how to handle this crosstalk. Obviously, one can no longer treat the color planes as if they are independent and contain only information about one velocity channel. Crosstalk between color channels shows up in the correlation map as a zero velocity peak that if sufficiently strong, can bias the velocity data. Two approaches have been used to minimize the effect of crosstalk. The first is to subtract a portion of the bleeding color channel (blue image) from the channel being bleed into (green) before cross correlation occurs. The second is to mask the central peak of the correlation map before searching for the real correlation peak. The latter approach functions most efficiently when non-zero velocities are expected. Both approaches are effective for small crosstalk (less than 30%). Above this value crosstalk becomes very problematic.

If one can calibrate the LED emission with respect to the camera sensitivity, the crosstalk problem can be handled by directly solving for the various components. The total red-, green-, and blue-pixel values can be written as follows:

$$\begin{aligned} R_p &= r_r R + g_r G + b_r B \\ G_p &= r_g R + g_g G + b_g B \\ B_p &= r_b R + g_b G + b_b B \end{aligned} \quad (4)$$

where R_p , G_p , B_p are the total measured red, green, and blue pixel values, respectively, the coefficient b_i correspond to the % blue in the red channel, etc., and R , G , and B are the red, green and blue LED emission values, respectively. In Eq. (4) if no crosstalk occurs between channels, all cross-color coefficients (g_r , g_b , r_g , r_b , b_g , b_r) will have a zero value. If the coefficients are known and the pixel values measured, then there are three equations in three unknowns, which can be readily solved for the original red, green, and blue LED values. Take a simpler case as an example; if one uses only the blue and green LEDs, Eq. (4) can be simplified to

$$\begin{aligned} G_p &= g_g G + b_g B \\ B_p &= g_b G + b_b B \end{aligned} \quad (5)$$

which has the following solution:

$$B = \frac{(g_g - 1)G_p + g_g B_p}{b_b + g_g - 1} \quad \text{and} \quad G = \frac{G_p}{g_g} - \frac{1 - b_b}{g_g} B \quad \text{where} \quad g_g \neq 1 - b_b \quad (6)$$

assuming that no blue or green light is lost to the red channel. Note the requirement that $g_g \neq 1 - b_b$ simply means that the two LEDs must have some difference in their spectral content that is measurable with the blue and green color filters. Therefore, despite the close spectral content of the LEDs, as long as they excite both the blue and green pixels in a slightly different manner, one should be able to solve for their original values employing Eq. (6). All that is needed for this solution is the color coefficients (obtained by a simple calibration procedure) and the individual blue- and green-pixel values; then using Eq. (6) one can determine the original blue and green values.

How close one can spectrally position the LEDs becomes a problem since they must be spatially overlapped for minimizing angular differences. A dichroic filter is typically used for this purpose; however, as a rule the sharper the cutoff frequency of the filter, the lower the transmission. One high-powered LED that excites both the blue and green pixels of the camera is cyan (480 nm) in color. The cyan LED potentially can be used with either the blue or green LEDs. The proximity of the blue and cyan emissions, however, makes it difficult to combine their outputs. Thus, combining the cyan and green LEDs will result in a minimization of several of the color problems discussed above including chromatic aberrations ($\Delta\lambda$ is small), color pixel density (it utilizes a high percentage of the camera pixels 75%), and color crosstalk (it displays sufficient spectral difference to permit Eq. (6) to be used to process the velocity data accurately).

top. Movies of the vector files indicate the flow had a lot of three-dimensional character (flow moving in and out of the plane of measurement).

B. Cylinder In Cross Flow Results.

A classic example of a dynamic flowfield is represented by a cylinder in cross flow. A small 3 mm diameter cylinder was positioned inside a 10 mm rectangular water flow channel and the color (blue-green) PSV images captured at a 500 Hz rate with the PCO 1200 camera. The time separation between blue and green pulses was 100 μ sec. Note with conventional PIV, the laser light sheet would have produced glare at the cylinder surface and the cylinder would have partly block the light sheet in the direction opposite to the incident light. The PSV approach, however, produced no glare nor had any regions blocked by the cylinder.

An example of raw PSV images that were obtained during this experiment is shown in Fig. 8a. The traditional and particle centric velocity vector maps from these images are shown in Figs. 8b and 8c, respectively. The water flow was from right to left in these images. The vortex shedding behind the cylinder is clearly visible. Note the difference between the traditional analysis and the particle centric analysis results, namely, the chaotic nature of the flow is much more evident in particle centric analysis.

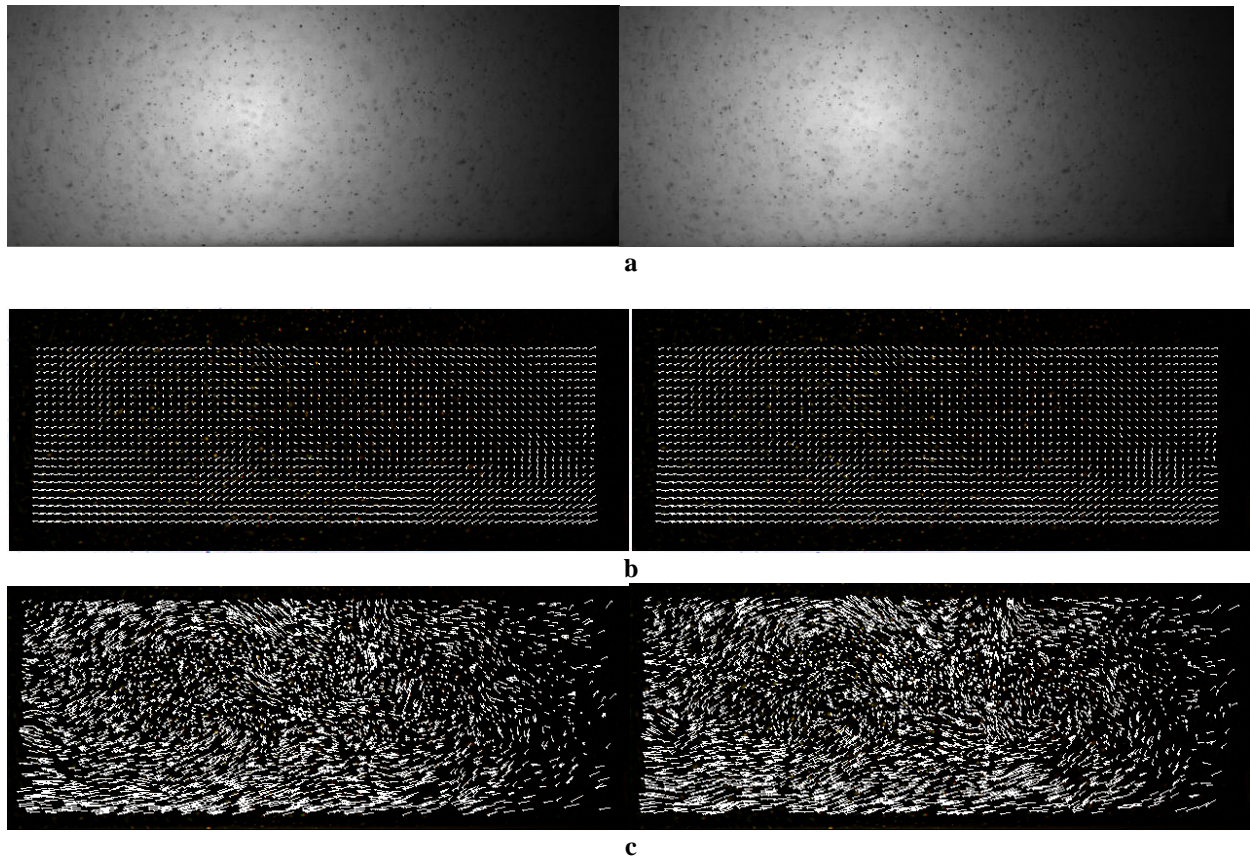


Figure 7. High Speed Cuvette Flow Captured by the PSV Technique. a) Raw PSV images taken at 0 (left) and 900 μ s (right), b) traditional PIV analysis results at 0 (left) and 900 μ s (right), and c) particle centric analysis results at 0 (left) and 900 μ s (right).

C. Artificial Heart Valve Results.

Dr. Fontain at Penn State University allowed us to make measurements on an artificial heart valve setup in his laboratory. The measurements were made using the high speed RGB LED lamp (using the blue and green LEDs) and the PCO 1200 color camera. Unfortunately it was not discovered until after the experiments were concluded that the time separation between the two colors was too short to be utilized for velocity analysis. The inter-frame time of 2 ms (PCO 1200 operated with a single ADC), however, was almost ideal for measurements in this flow. As a result the frame to frame green channels were processed for the velocity fields discussed below.

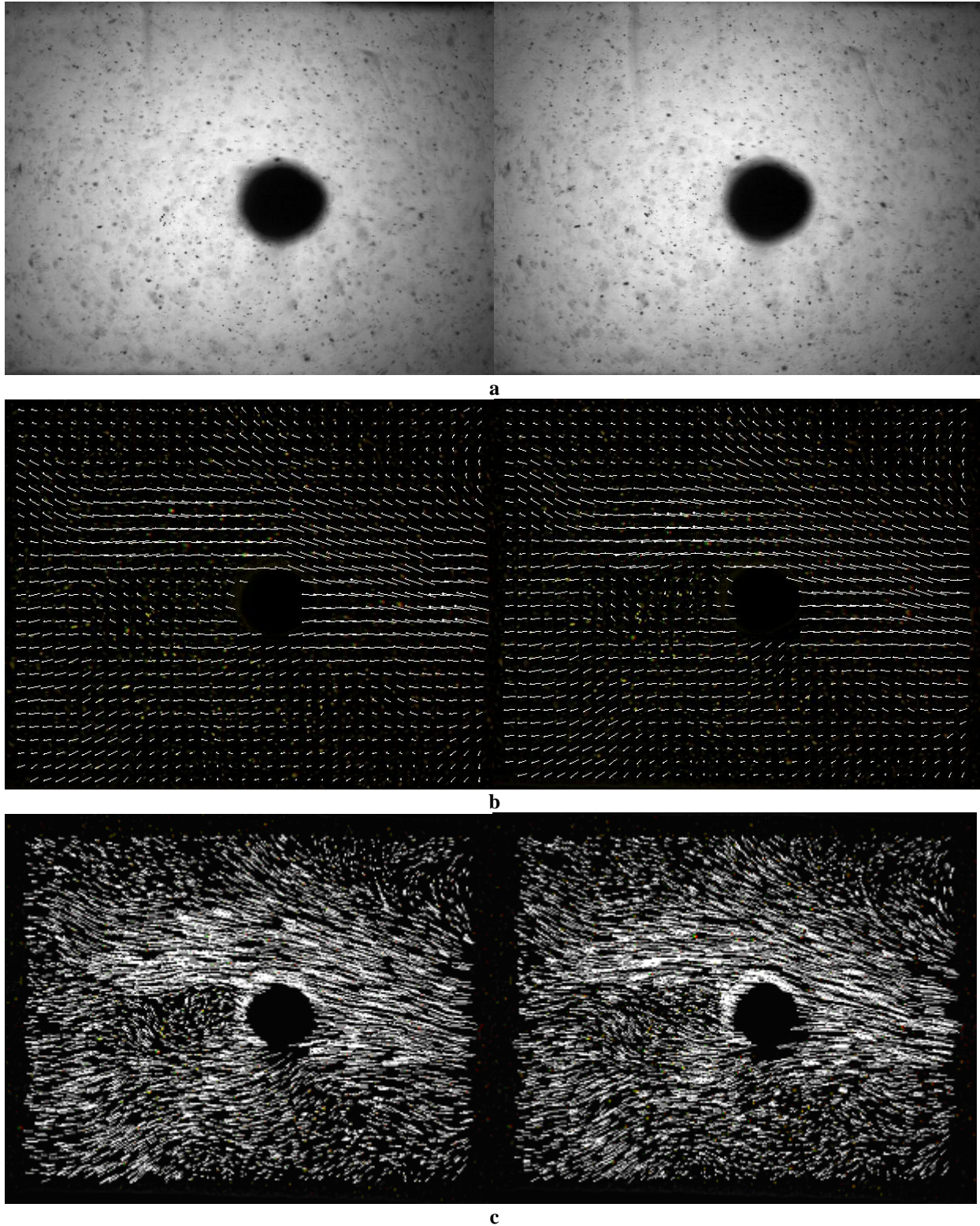


Figure 8. Velocity Measurements on a Cylinder in Cross Flow by the PSV Technique. a) Raw PSV images at time-0 (left) and 2 ms (right), b) resulting velocity fields by traditional PIV analysis at time 0 (left) and 2 ms (right), c) resulting velocity fields by particle centric analysis at time 0 (left) and 2 ms (right).

The heart valve velocity maps obtained at various times are shown in Fig. 9. Starting at a low velocity valve closed state (22 ms, Fig. 9a) we can see the flow is well organized with a vortex centered near the valve. Of note in this image is the evidence for backflow or leakage near the gap between the valve and wall (see the downward flow vectors near the upper left of the valve). Figure 9b shows the flow map at 250 ms just as the valve starts to open. The peak velocity with the valve open is observed at 460 ms as shown in Fig. 9c. The flowfield reverses direction starting at 502 ms (Fig. 9d) reaching a peak reverse flow velocity at 516 ms (Fig. 9e). Figure 9f (546 ms) shows the chaotic nature of the flow as the valve closes. Note some of the bad vectors shown in this figure are due to the velocities being too high for the inter-frame time separation. Figure 9g (738 ms) shows the flowfield ~ 200 ms later after it has slowed and become more organized. Figure 9h (1000 ms) is near the end of the pumping cycle. Note the absence of the vortex structure shown in Fig. 9a indicating there is some cycle to cycle variation in the flowfield.

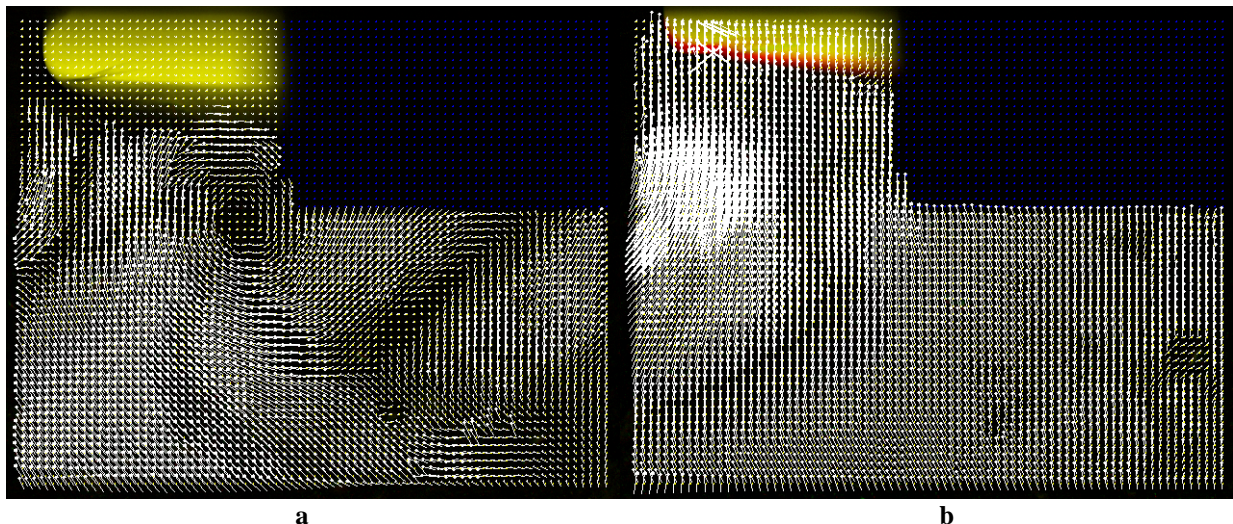
V. Conclusions

Particle Shadow Velocimetry (PSV) is a volumetric based velocimetry technique that utilizes collection optics to minimize the measurement depth. Imaging of calibrated circular discs indicate that the measurement depth of the technique can be substantially larger than that predicted for an optically equivalent epi-fluorescent microPIV system. The increased measurement volume is due to the partial coherence of the LED light sources used in the technique and the detection of forward scattering in addition to particle light extinction (shadows). It is shown that by introducing a spatial diffuser into the optical train upstream of the measurement volume, the measurement depth can be improved. The added step of squaring the PSV image brings the measurement depth to within a factor of two of that predicted for microPIV. The application of the technique to color requires that several potential problems be addressed including: chromatic aberrations, color crosstalk, and non-uniform color camera pixel distribution. It is shown that each of these problems can be addressed by utilizing LEDs that are spatially aligned and spectrally adjacent to color camera filter cut-offs (blue-green edge or green-red edge). It is also demonstrated that allowing crosstalk to occur with the green color plane improves the spatial information of both the blue and red color planes.

A high power pulsed RGB LED lamp system has been developed that in conjunction with a high-speed PCO color camera allows velocity measurements in excess of a kilohertz to be obtained. Experimental measurements were made in a cuvette flow, a cylinder in cross flow and an artificial heart valve. The analysis of these flows with traditional PIV cross-correlation and particle centric approaches reveals the complex nature of these flowfields.

Acknowledgements

The help of B. Sarka, G. Webb, and D. Trump of Innovative Scientific Solutions, Inc., in the design and fabrication of the LED clusters and PSV instrument is gratefully acknowledged. Special thanks to Dr. Arnie Fontain at Penn State University for us of his artificial heart valve setup.



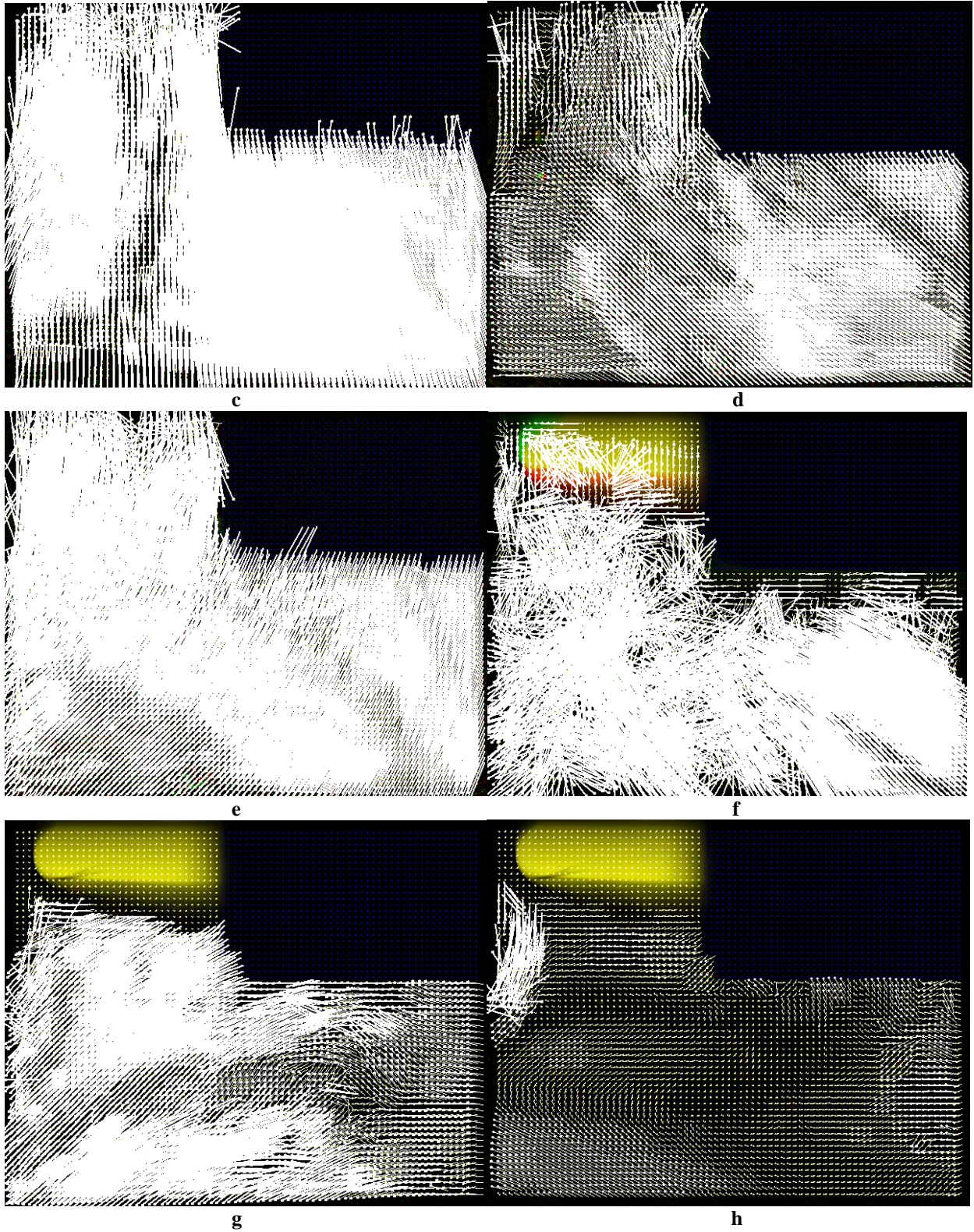


Figure. 9 Velocity Fields of Flow Behind an Artificial Heart Value Obtained with PSV Technique. Vectors at time a) 22 ms b) 250 ms, c) 460 ms, d) 502 ms, e) 516 ms, f) 546 ms, g) 738 ms, and h) 1000 ms.

References

1. Esteveordal, J. and L. P. Goss, "PIV with LED: particle shadow velocimetry (PSV) technique," AIAA Paper 2005-0037, Reno, NV, Jan 10-13, 2005.
2. Esteveordal, J., and L. P. Goss, "An investigation of particle shadow velocimetry (PSV) for transonic flow applications," AIAA Paper 2005-5009, Toronto, Canada, June 6-9, 2005.
3. Santiago, J. G., Wereley, S. T., Meinhart, C. D., Beebe, D. J., and R. J. Adrian, "A particle image velocimetry system for microfluidics," *Exp. Fluids* **25** 316-319, 1998.
4. Meinhart, C. D. and H. Zhang, "The flow structure inside a microfabricated inkjet printhead," *J. Microelectromech. Syst.* **9** 67-75, 2000.
5. Tretheway D. C., and C. D. Meinhart, "Apparent fluid slip at hydrophobic microchannel walls," *Phys. Fluids* **14** L9-12, 2002.
6. Ovrn, B., Hallinan, K., and K. Das, "Quantative three-dimensional flow in a microscopic field of view," FEDSM98-5268, 1998 ASME Fluids Engineering Division Summer Meeting, Washington, D.C., June 21-25, 1998.
7. Ovrn, B. and S. H. Izen, "Imaging of transparent spheres through a planar interface using a high-numerical-aperture optical microscope," *J. Opt. Soc. Am. A*, **17** 1202-1213, 2000.
8. van de Hulst, H. C., "Light Scattering by Small Particles," Wiley, New York, 1957.
9. Meinhart, C. D., Wereley, S. T., and M. H. B. Gray, "Volume illumination for two-dimensional particle image velocimetry," *Meas. Sci. Technol.* **11** 809-814, 2000.
10. Olsen, M. G. and R. J. Adrian, "Out of focus effects on particle image visibility and correlation in microscopic particle image velocimetry," *Exps. Fluids* **29** (Suppl.) S166-174, 2000.
11. Bourdon, C. J., Olsen, M. G., and A. D. Gorby, "Validation of an analytical solution for depth of correlation in microscopic particle image velocimetry," *Meas. Sci. Technol.* **15**, 318-327, 2004.
12. Olsen, M. G., Bourdon, C. J., and A. D. Gorby, "Power filtering technique for modifying depth of correlation in microPIV experiments," 11th International Symposium on Flow Visualization, South Bend, IN, Aug. 9-12, 2004.
13. Bayer, B. E., "Color Imaging Array," US Patent No. 3971065.
14. Nussenzveig, H. M., "Diffraction Effects in Semiclassical Scattering," Cambridge University Press, Great Britian.